

RECOMMENDATION ITU-R P.526-9

Propagation by diffraction

(Question ITU-R 202/3)

(1978-1982-1992-1994-1995-1997-1999-2001-2003-2005)

The ITU Radiocommunication Assembly,

considering

a) that there is a need to provide engineering information for the calculation of field strengths over diffraction paths,

recommends

1 that the methods described in Annex 1 be used for the calculation of field strengths over diffraction paths, which may include a spherical earth surface, or irregular terrain with different kinds of obstacles.

Annex 1**1 Introduction**

Although diffraction is produced only by the surface of the ground or other obstacles, account must be taken of the mean atmospheric refraction on the transmission path to evaluate the geometrical parameters situated in the vertical plane of the path (angle of diffraction, radius of curvature, height of obstacle). For this purpose, the path profile has to be traced with the appropriate equivalent Earth radius (Recommendation ITU-R P.834). If no other information is available, an equivalent Earth radius of 8 500 km may be taken as a basis.

2 Basic concepts

Diffraction of radiowaves over the Earth's surface is affected by terrain irregularities. In this context, before going further into the prediction methods for this propagation mechanism, a few basic concepts are given in this section.

2.1 Fresnel ellipsoids and Fresnel zones

In studying radiowave propagation between two points A and B, the intervening space can be subdivided by a family of ellipsoids, known as Fresnel ellipsoids, all having their focal points at A and B such that any point M on one ellipsoid satisfies the relation:

$$AM + MB = AB + n \frac{\lambda}{2} \quad (1)$$

where n is a whole number characterizing the ellipsoid and $n = 1$ corresponds to the first Fresnel ellipsoid, etc., and λ is the wavelength.

As a practical rule, propagation is assumed to occur in line-of-sight (LoS), i.e. with negligible diffraction phenomena if there is no obstacle within the first Fresnel ellipsoid.

The radius of an ellipsoid at a point between the transmitter and the receiver can be approximated by:

$$R_n = \left[\frac{n \lambda d_1 d_2}{d_1 + d_2} \right]^{1/2} \quad (2)$$

or, in practical units:

$$R_n = 550 \left[\frac{n d_1 d_2}{(d_1 + d_2) f} \right]^{1/2} \quad (3)$$

where f is the frequency (MHz) and d_1 and d_2 are the distances (km) between transmitter and receiver at the point where the ellipsoid radius (m) is calculated.

Some problems require consideration of Fresnel zones which are the zones obtained by taking the intersection of a family of ellipsoids by a plane. The zone of order n is the part between the curves obtained from ellipsoids n and $n - 1$, respectively.

2.2 Penumbra width

The transition from light to shadow defines the penumbra region. This transition takes place along a narrow strip (penumbra width) in the boundary of geometric shadow. Figure 1 shows the penumbra width (W) in the case of a transmitter located a height, h , above a smooth spherical earth, which is given by:

$$w = \left[\frac{\lambda a_e^2}{\pi} \right]^{1/3} \quad \text{m} \quad (4)$$

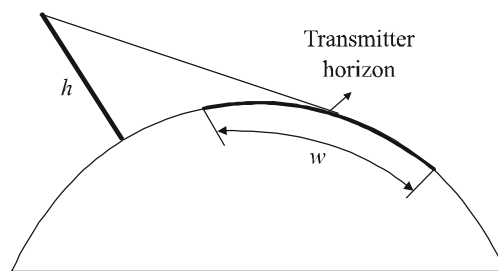
where:

λ : wavelength (m)

a_e : effective Earth radius (m).

FIGURE 1

Definition of penumbra width



0526-01

2.3 Diffraction zone

The diffraction zone of a transmitter extends from the LoS distance where the path clearance is equal to 60% of the first Fresnel zone radius, (R_1), up to a distance well beyond the transmitter horizon where the mechanism of troposcatter becomes predominant.

2.4 Obstacle surface smoothness criterion

If the surface of the obstacle has irregularities not exceeding Δh ,
where:

$$\Delta h = 0.04 [R\lambda^2]^{1/3} \quad \text{m} \quad (5)$$

where:

R : obstacle curvature radius (m)

λ : wavelength (m)

then the obstacle may be considered smooth and the methods described in § 3 and 4.2 may be used to calculate the attenuation.

2.5 Isolated obstacle

An obstacle can be considered isolated if there is no interaction between the obstacle itself and the surrounding terrain. In other words, the path attenuation is only due to the obstacle alone without any contribution from the remaining terrain. The following conditions must be satisfied:

- no overlapping between penumbra widths associated with each terminal and the obstacle top;
- the path clearance on both sides of the obstacles should be, at least, 0.6 of the first Fresnel zone radius;
- no specular reflection on both sides of the obstacle.

2.6 Types of terrain

Depending on the numerical value of the parameter Δh (see Recommendation ITU-R P.310) used to define the degree of terrain irregularities, three types of terrain can be classified:

a) *Smooth terrain*

The surface of the Earth can be considered smooth if terrain irregularities are of the order or less than $0.1R$, where R is the maximum value of the first Fresnel zone radius in the propagation path. In this case, the prediction model is based on the diffraction over the spherical Earth (§ 3).

b) *Isolated obstacles*

The terrain profile of the propagation path consists of one or more isolated obstacles. In this case, depending on the idealization used to characterize the obstacles encountered in the propagation path, the prediction models described in § 4 should be used.

c) *Rolling terrain*

The profile consists of several small hills, none of which form a dominant obstruction. Within its frequency range Recommendation ITU-R P.1546 is suitable for predicting field strength but it is not a diffraction method.

2.7 Fresnel integrals

The complex Fresnel integral is given by:

$$F_c(v) = \int_0^v \exp\left(j \frac{\pi s^2}{2}\right) ds = C(v) + jS(v) \quad (6)$$

where j is the complex operator equal to $\sqrt{-1}$, and $C(v)$ and $S(v)$ are the Fresnel cosine and sine integrals defined by:

$$C(v) = \int_0^v \cos\left(\frac{\pi s^2}{2}\right) ds \quad (7a)$$

$$S(v) = \int_0^v \sin\left(\frac{\pi s^2}{2}\right) ds \quad (7b)$$

The complex Fresnel integral $F_c(v)$ can be evaluated by numerical integration, or with sufficient accuracy for most purposes for positive v using:

$$F_c(v) = \exp(jx) \sqrt{\frac{x}{4}} \sum_{n=0}^{11} \left[(a_n - jb_n) \left(\frac{x}{4}\right)^n \right] \quad \text{for } 0 \leq x < 4 \quad (8a)$$

$$F_c(v) = \left(\frac{1+j}{2}\right) \exp(jx) \sqrt{\frac{4}{x}} \sum_{n=0}^{11} \left[(c_n - jd_n) \left(\frac{4}{x}\right)^n \right] \quad \text{for } x \geq 4 \quad (8b)$$

where:

$$x = 0.5 \pi v^2 \quad (9)$$

and a_n , b_n , c_n and d_n are the Boersma coefficients given below:

$a_0 = +1.595769140$	$b_0 = -0.000000033$	$c_0 = +0.000000000$	$d_0 = +0.199471140$
$a_1 = -0.000001702$	$b_1 = +4.255387524$	$c_1 = -0.024933975$	$d_1 = +0.000000023$
$a_2 = -6.808568854$	$b_2 = -0.000092810$	$c_2 = +0.000003936$	$d_2 = -0.009351341$
$a_3 = -0.000576361$	$b_3 = -7.780020400$	$c_3 = +0.005770956$	$d_3 = +0.000023006$
$a_4 = +6.920691902$	$b_4 = -0.009520895$	$c_4 = +0.000689892$	$d_4 = +0.004851466$
$a_5 = -0.016898657$	$b_5 = +5.075161298$	$c_5 = -0.009497136$	$d_5 = +0.001903218$
$a_6 = -3.050485660$	$b_6 = -0.138341947$	$c_6 = +0.011948809$	$d_6 = -0.017122914$
$a_7 = -0.075752419$	$b_7 = -1.363729124$	$c_7 = -0.006748873$	$d_7 = +0.029064067$
$a_8 = +0.850663781$	$b_8 = -0.403349276$	$c_8 = +0.000246420$	$d_8 = -0.027928955$
$a_9 = -0.025639041$	$b_9 = +0.702222016$	$c_9 = +0.002102967$	$d_9 = +0.016497308$
$a_{10} = -0.150230960$	$b_{10} = -0.216195929$	$c_{10} = -0.001217930$	$d_{10} = -0.005598515$
$a_{11} = +0.034404779$	$b_{11} = +0.019547031$	$c_{11} = +0.000233939$	$d_{11} = +0.000838386$

$C(v)$ and $S(v)$ may be evaluated for negative values of v by noting that:

$$C(-v) = -C(v) \quad (10a)$$

$$S(-v) = -S(v) \quad (10b)$$

3 Diffraction over a spherical Earth

The additional transmission loss due to diffraction over a spherical Earth can be computed by the classical residue series formula. A computer program GRWAVE, available from the ITU, provides the complete method. A subset of the outputs from this program (for antennas close to the ground and at lower frequencies) is presented in Recommendation ITU-R P.368.

3.1 Diffraction loss for over-the-horizon paths

At long distances over the horizon, only the first term of the residue series is important. Even near or at the horizon this approximation can be used with a maximum error around 2 dB in most cases.

This first term can be written as the product of a distance term, F , and two height gain terms, G_T and G_R . § 3.1.1 and § 3.1.2 describe how these terms can be obtained from simple formula or from nomograms.

3.1.1 Numerical calculation

3.1.1.1 Influence of the electrical characteristics of the surface of the Earth

The extent to which the electrical characteristics of the surface of the Earth influence the diffraction loss can be determined by calculating a normalized factor for surface admittance, K , given by the formulae:

in self-consistent units:

$$K_H = \left(\frac{2\pi a_e}{\lambda} \right)^{-1/3} \left[(\epsilon - 1)^2 + (60\lambda\sigma)^2 \right]^{-1/4} \quad \text{for horizontal polarization} \quad (11)$$

and

$$K_V = K_H \left[\epsilon^2 + (60\lambda\sigma)^2 \right]^{1/2} \quad \text{for vertical polarization} \quad (12)$$

or, in practical units:

$$K_H = 0.36(a_e f)^{-1/3} \left[(\epsilon - 1)^2 + (18000\sigma/f)^2 \right]^{-1/4} \quad (11a)$$

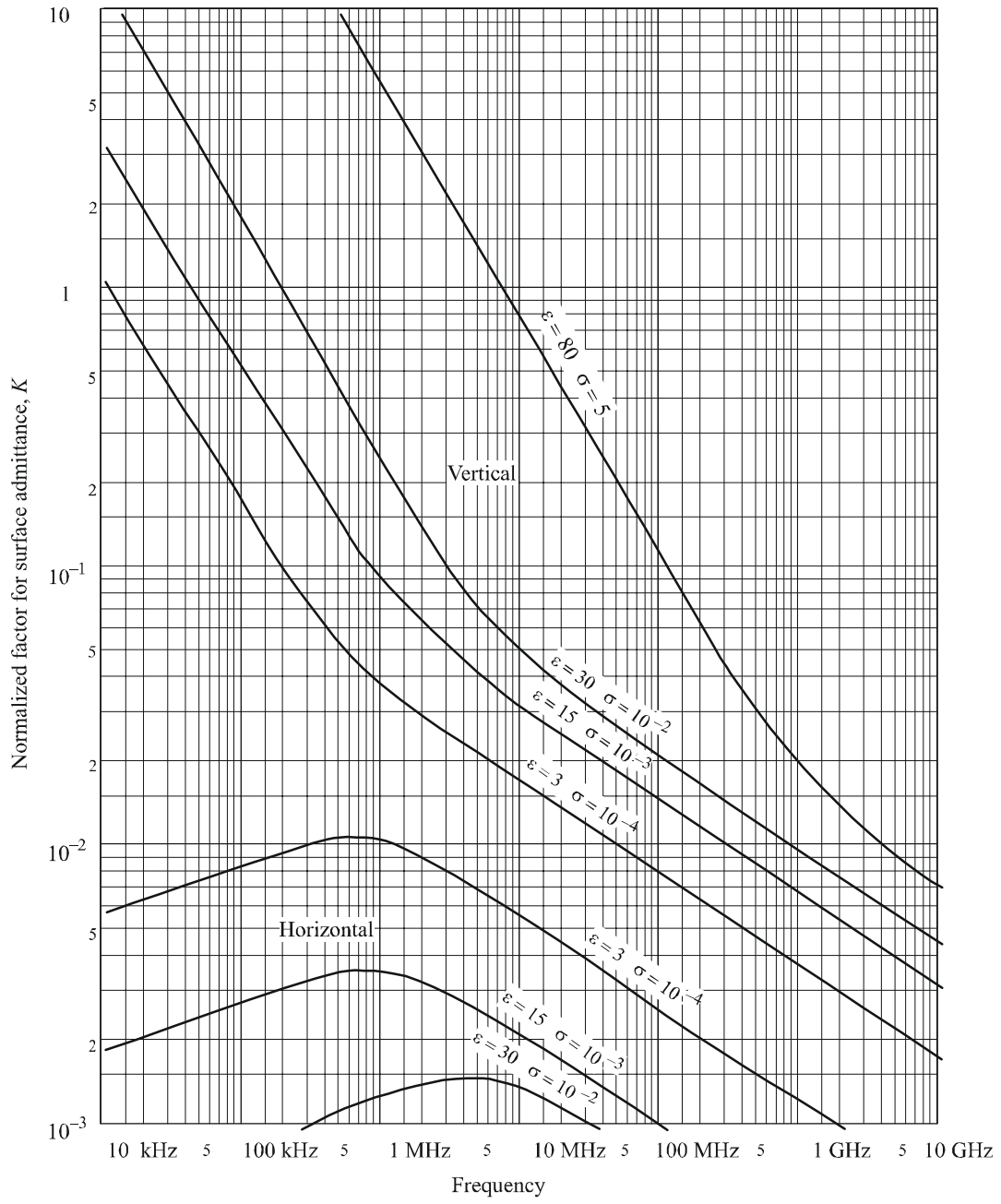
$$K_V = K_H \left[\epsilon^2 + (18000\sigma/f)^2 \right]^{1/2} \quad (12a)$$

where:

- a_e : effective radius of the Earth (km)
- ϵ : effective relative permittivity
- σ : effective conductivity (S/m)
- f : frequency (MHz).

Typical values of K are shown in Fig. 2.

FIGURE 2
Calculation of K



If K is less than 0.001, the electrical characteristics of the Earth are not important. For values of K greater than 0.001, the appropriate formulae given below should be used.

3.1.1.2 Diffraction field strength formulae

The diffraction field strength, E , relative to the free-space field strength, E_0 , is given by the formula:

$$20 \log \frac{E}{E_0} = F(X) + G(Y_1) + G(Y_2) \quad \text{dB} \quad (13)$$

where X is the normalized length of the path between the antennas at normalized heights Y_1 and Y_2 (and where $20 \log \frac{E}{E_0}$ is generally negative).

In self-consistent units:

$$X = \beta \left(\frac{\pi}{\lambda a_e^2} \right)^{1/3} d \quad (14)$$

$$Y = 2\beta \left(\frac{\pi^2}{\lambda^2 a_e} \right)^{1/3} h \quad (15)$$

or, in practical units:

$$X = 2.2\beta f^{1/3} a_e^{-2/3} d \quad (14a)$$

$$Y = 9.6 \times 10^{-3} \beta f^{2/3} a_e^{-1/3} h \quad (15a)$$

where:

- d : path length (km)
- a_e : equivalent Earth's radius (km)
- h : antenna height (m)
- f : frequency (MHz).

β is a parameter allowing for the type of ground and for polarization. It is related to K by the following semi-empirical formula:

$$\beta = \frac{1 + 1.6K^2 + 0.75K^4}{1 + 4.5K^2 + 1.35K^4} \quad (16)$$

For horizontal polarization at all frequencies, and for vertical polarization above 20 MHz over land or 300 MHz over sea, β may be taken as equal to 1.

For vertical polarization below 20 MHz over land or 300 MHz over sea, β must be calculated as a function of K . However, it is then possible to disregard ε and write:

$$K^2 \approx 6.89 \frac{\sigma}{k^{2/3} f^{5/3}} \quad (16a)$$

where σ is expressed in S/m, f (MHz) and k is the multiplying factor of the Earth's radius.

The distance term is given by the formula:

$$F(X) = 11 + 10 \log(X) - 17.6 X \quad (17)$$

The height gain term, $G(Y)$ is given by the following formulae:

$$G(Y) \cong 17.6(Y - 1.1)^{1/2} - 5 \log(Y - 1.1) - 8 \quad \text{for } Y > 2 \quad (18)$$

For $Y < 2$ the value of $G(Y)$ is a function of the value of K computed in § 3.1.1:

$$G(Y) \cong 20 \log(Y + 0.1Y^3) \quad \text{for } 10K < Y < 2 \quad (18a)$$

$$G(Y) \cong 2 + 20 \log K + 9 \log(Y/K) [\log(Y/K) + 1] \quad \text{for } K/10 < Y < 10K \quad (18b)$$

$$G(Y) \cong 2 + 20 \log K \quad \text{for } Y < K/10 \quad (18c)$$

3.1.2 Calculation by nomograms

Under the same approximation condition (the first term of the residue series is dominant), the calculation may also be made using the following formula:

$$20 \log \frac{E}{E_0} = F(d) + H(h_1) + H(h_2) \quad \text{dB} \quad (19)$$

where:

E : received field strength

E_0 : field strength in free space at the same distance

d : distance between the extremities of the path

h_1 and h_2 : heights of the antennas above the spherical earth.

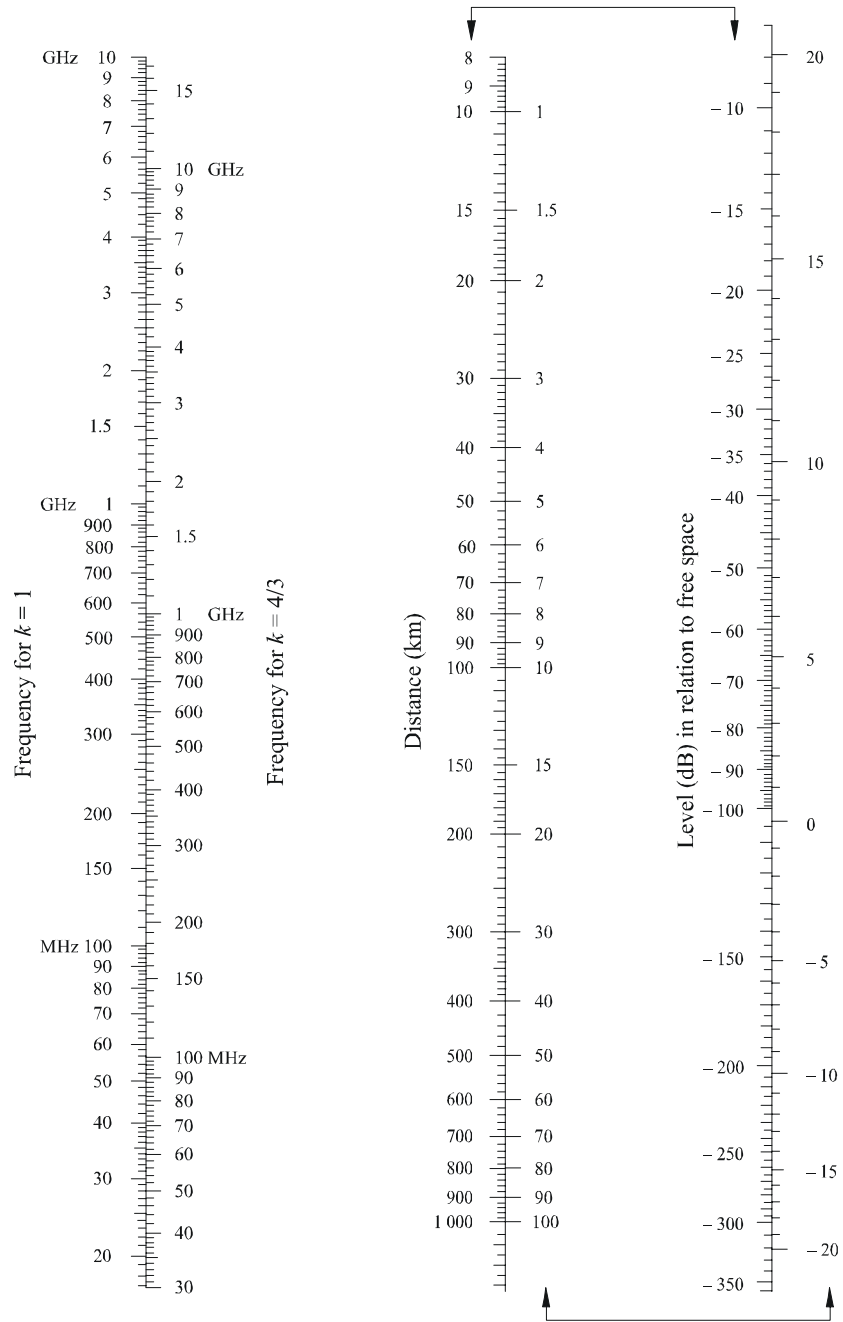
The function F (influence of the distance) and H (height-gain) are given by the nomograms in Figs. 3, 4, 5 and 6.

These nomograms (Figs. 3 to 6) give directly the received level relative to free space, for $k = 1$ and $k = 4/3$, and for frequencies greater than approximately 30 MHz. k is the effective Earth radius factor, defined in Recommendation ITU-R P.310. However, the received level for other values of k may be calculated by using the frequency scale for $k = 1$, but replacing the frequency in question by a hypothetical frequency equal to f/k^2 for Figs. 3 and 5 and f/\sqrt{k} , for Figs. 4 and 6.

Very close to the ground the field strength is practically independent of the height. This phenomenon is particularly important for vertical polarization over the sea. For this reason Fig. 6 includes a heavy black vertical line AB. If the straight line should intersect this heavy line AB, the real height should be replaced by a larger value, so that the straight line just touches the top of the limit line at A.

NOTE 1 – Attenuation relative to free space is given by the negative of the values given by equation (19). If equation (19) gives a value above the free-space field, the method is invalid.

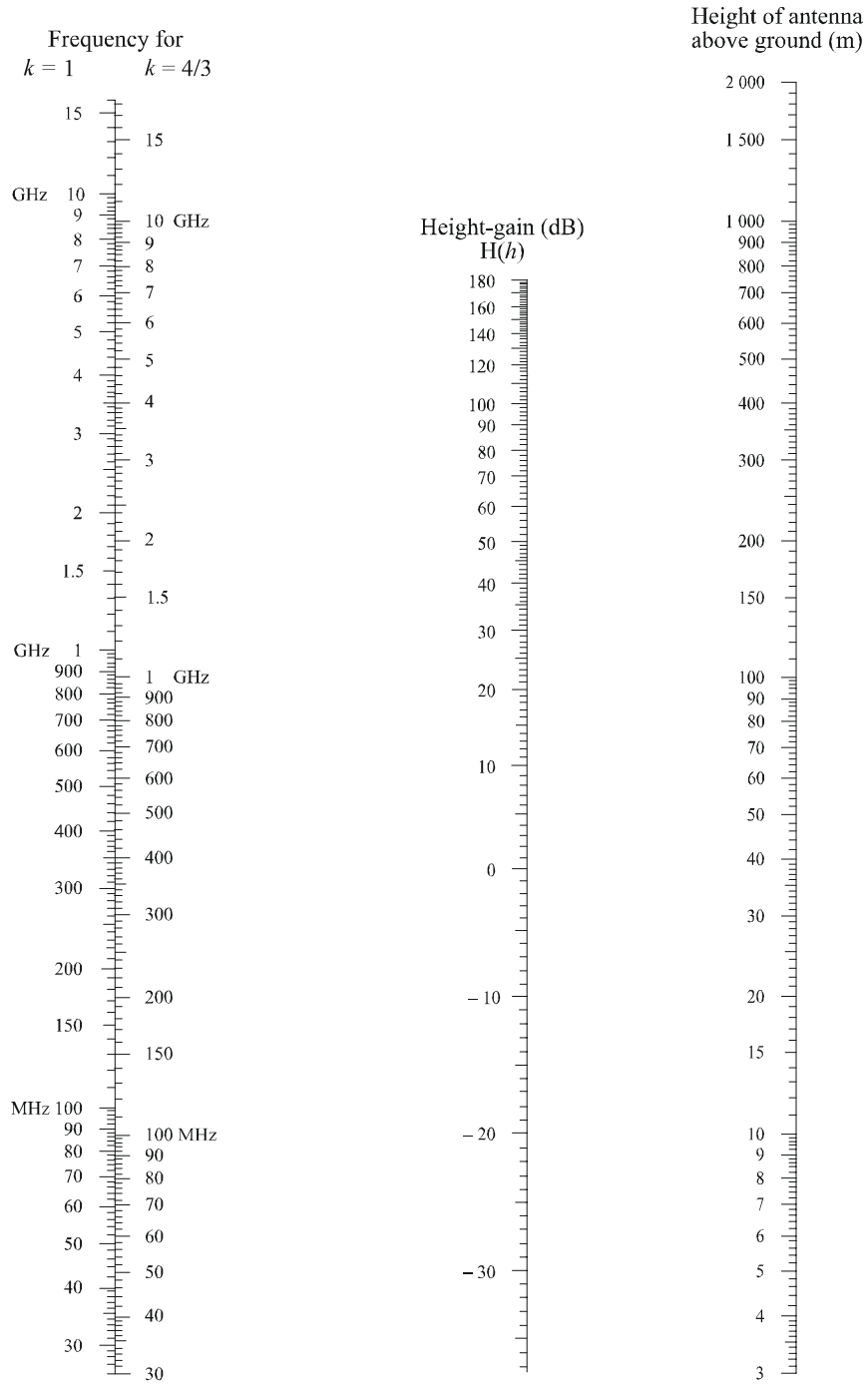
FIGURE 3
 Diffraction by a spherical Earth – effect of distance



Horizontal polarization over land and sea
 Vertical polarization over land

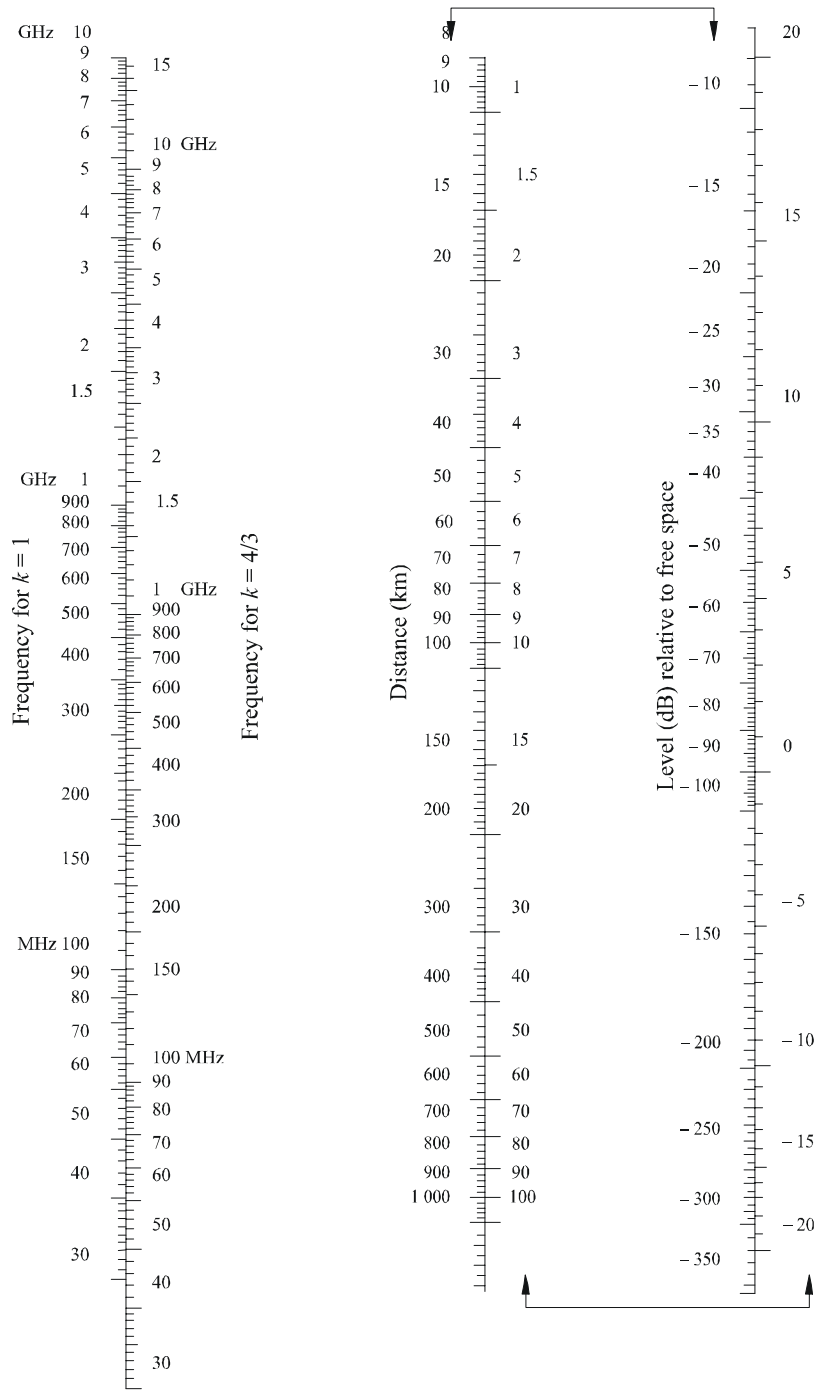
(The scales joined by arrows should be used together)

FIGURE 4
 Diffraction by a spherical Earth – height-gain



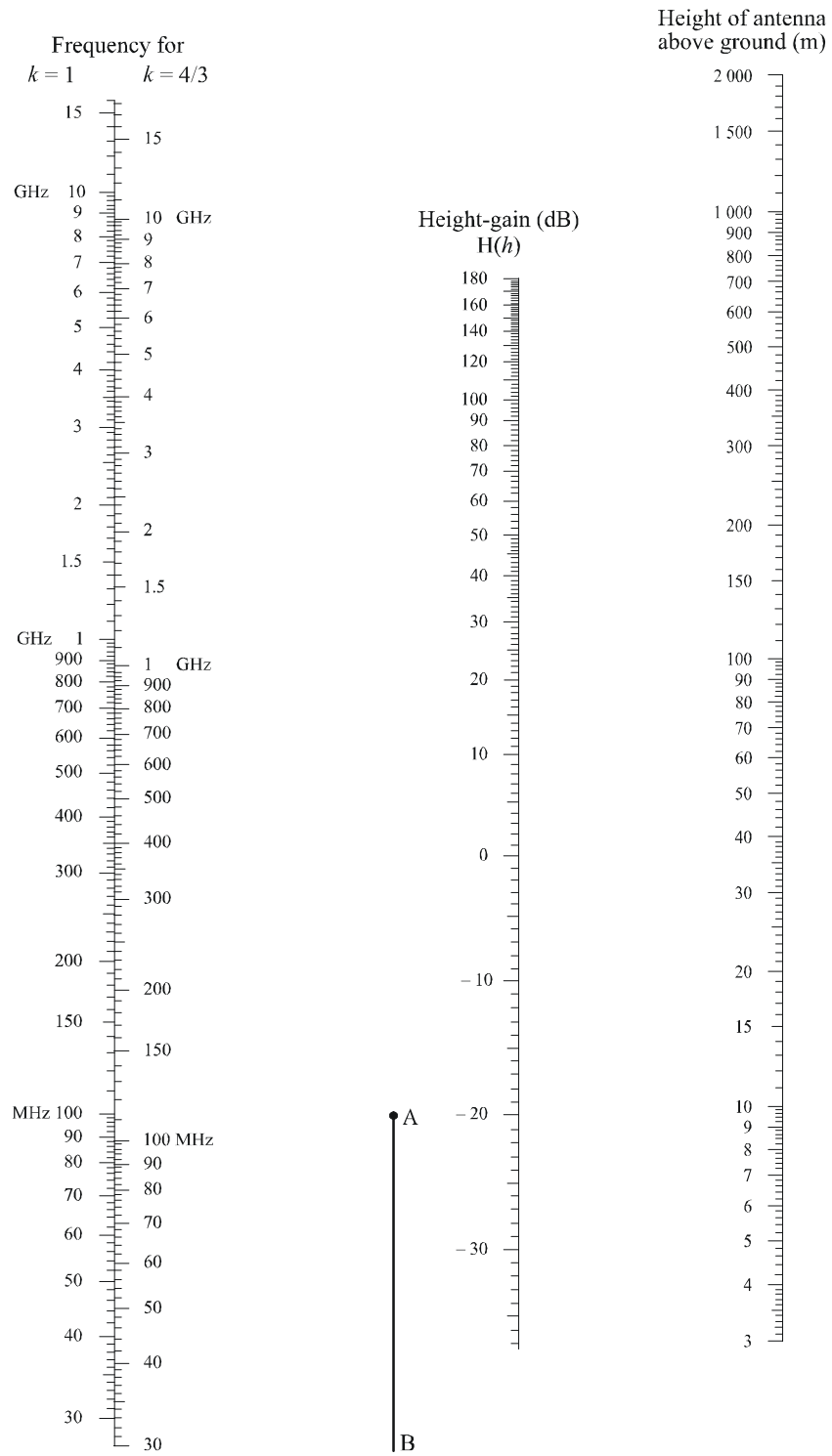
Horizontal polarization – land and sea
 Vertical polarization – land

FIGURE 5
 Diffraction by a spherical Earth – effect of distance



Vertical polarization over sea
 (The scales joined by arrows should be used together)

FIGURE 6
Diffraction by a spherical Earth – height-gain



Vertical polarization – sea

3.2 Diffraction loss for LoS paths with sub-path diffraction

In this case, considering that the convergence of the residue series requires the calculation of several terms, a linear interpolation between the limit of diffraction zone (clearance of 0.6 of the first Fresnel zone radius) where the attenuation relative to free-space is zero and the radio horizon can be used. According to this procedure, the diffraction loss is computed in terms of the first Fresnel zone radius, R_1 , as:

$$A(\text{dB}) = \left[1 - \frac{5}{3} \frac{h}{R_1} \right] A_h \quad (20)$$

where:

h : path clearance

A_h : diffraction loss at the horizon (see § 3.1).

The path clearance is given by (see Fig. 7):

$$h = \frac{\left(h_1 - \frac{d_1^2}{2a_e} \right) d_2 + \left(h_2 - \frac{d_2^2}{2a_e} \right) d_1}{d} \quad (21)$$

where:

$$d_1 = \frac{d}{2} (1 + b) \quad (21a)$$

$$d_2 = d - d_1 \quad (21b)$$

$$b = 2\sqrt{\frac{m+1}{3m}} \cos \left\{ \frac{\pi}{3} + \frac{1}{3} \arccos \left(\frac{3c}{2} \sqrt{\frac{3m}{(m+1)^3}} \right) \right\} \quad (21c)$$

$$c = \frac{|h_1 - h_2|}{h_1 + h_2} \quad (21d)$$

$$m = \frac{d^2}{4a_e(h_1 + h_2)} \quad (21e)$$

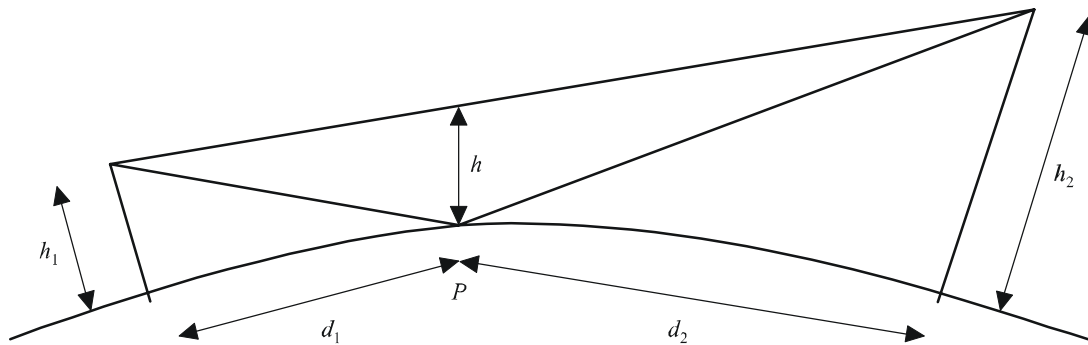
4 Diffraction over isolated obstacles

Many propagation paths encounter one obstacle or several separate obstacles and it is useful to estimate the losses caused by such obstacles. To make such calculations it is necessary to idealize the form of the obstacles, either assuming a knife-edge of negligible thickness or a thick smooth obstacle with a well-defined radius of curvature at the top. Real obstacles have, of course, more complex forms, so that the indications provided in this Recommendation should be regarded only as an approximation.

In those cases where the direct path between the terminals is much shorter than the diffraction path, it is necessary to calculate the additional transmission loss due to the longer path.

The data given below apply when the wavelength is fairly small in relation to the size of the obstacles, i.e., mainly to VHF and shorter waves ($f > 30$ MHz).

FIGURE 7
Path clearance



P: Reflection point

0526-07

4.1 Single knife-edge obstacle

In this extremely idealized case (Figs. 8a) and 8b)), all the geometrical parameters are combined together in a single dimensionless parameter normally denoted by v which may assume a variety of equivalent forms according to the geometrical parameters selected:

$$v = h \sqrt{\frac{2}{\lambda} \left(\frac{1}{d_1} + \frac{1}{d_2} \right)} \quad (22)$$

$$v = \theta \sqrt{\frac{2}{\lambda \left(\frac{1}{d_1} + \frac{1}{d_2} \right)}} \quad (23)$$

$$v = \sqrt{\frac{2h\theta}{\lambda}} \quad (v \text{ has the sign of } h \text{ and } \theta) \quad (24)$$

$$v = \sqrt{\frac{2d}{\lambda} \cdot \alpha_1 \alpha_2} \quad (v \text{ has the sign of } \alpha_1 \text{ and } \alpha_2) \quad (25)$$

where:

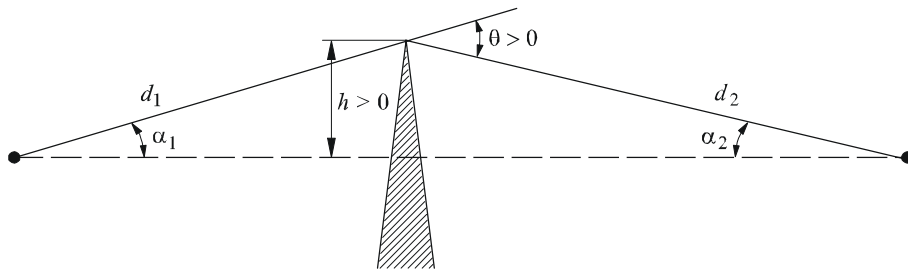
- h : height of the top of the obstacle above the straight line joining the two ends of the path. If the height is below this line, h is negative
- d_1 and d_2 : distances of the two ends of the path from the top of the obstacle
- d : length of the path
- θ : angle of diffraction (rad); its sign is the same as that of h . The angle θ is assumed to be less than about 0.2 rad, or roughly 12°
- α_1 and α_2 : angles between the top of the obstacle and one end as seen from the other end. α_1 and α_2 are of the sign of h in the above equations.

NOTE 1 – In equations (22) to (25) inclusive h , d , d_1 , d_2 and γ should be in self-consistent units.

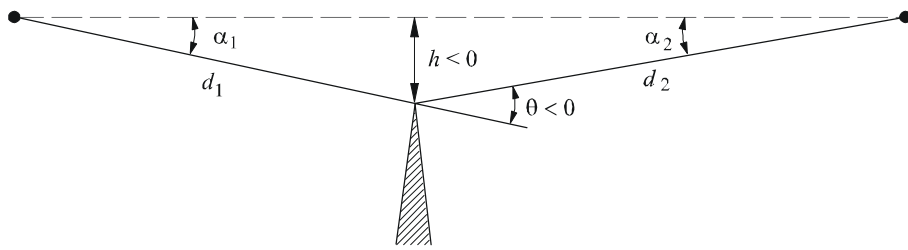
FIGURE 8

Geometrical elements

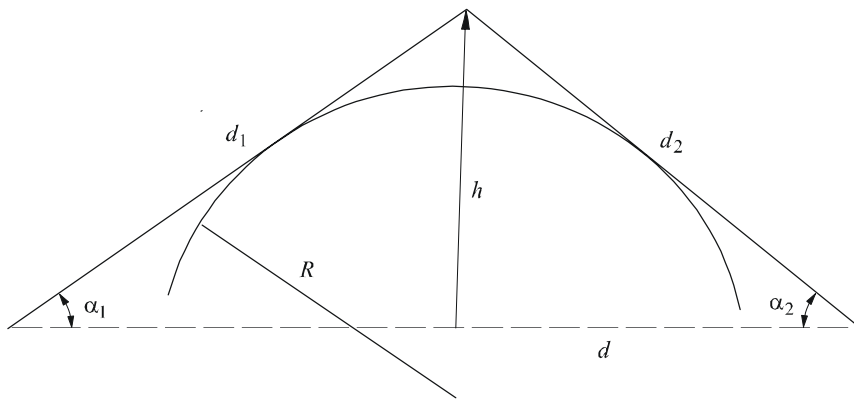
(For definitions of θ , α_1 , α_2 , d , d_1 , d_2 and R , see § 4.1 and 4.2)



a)



b)



c)

0526-08

Figure 9 gives, as a function of v , the loss $J(v)$ (dB).

$J(v)$ is given by:

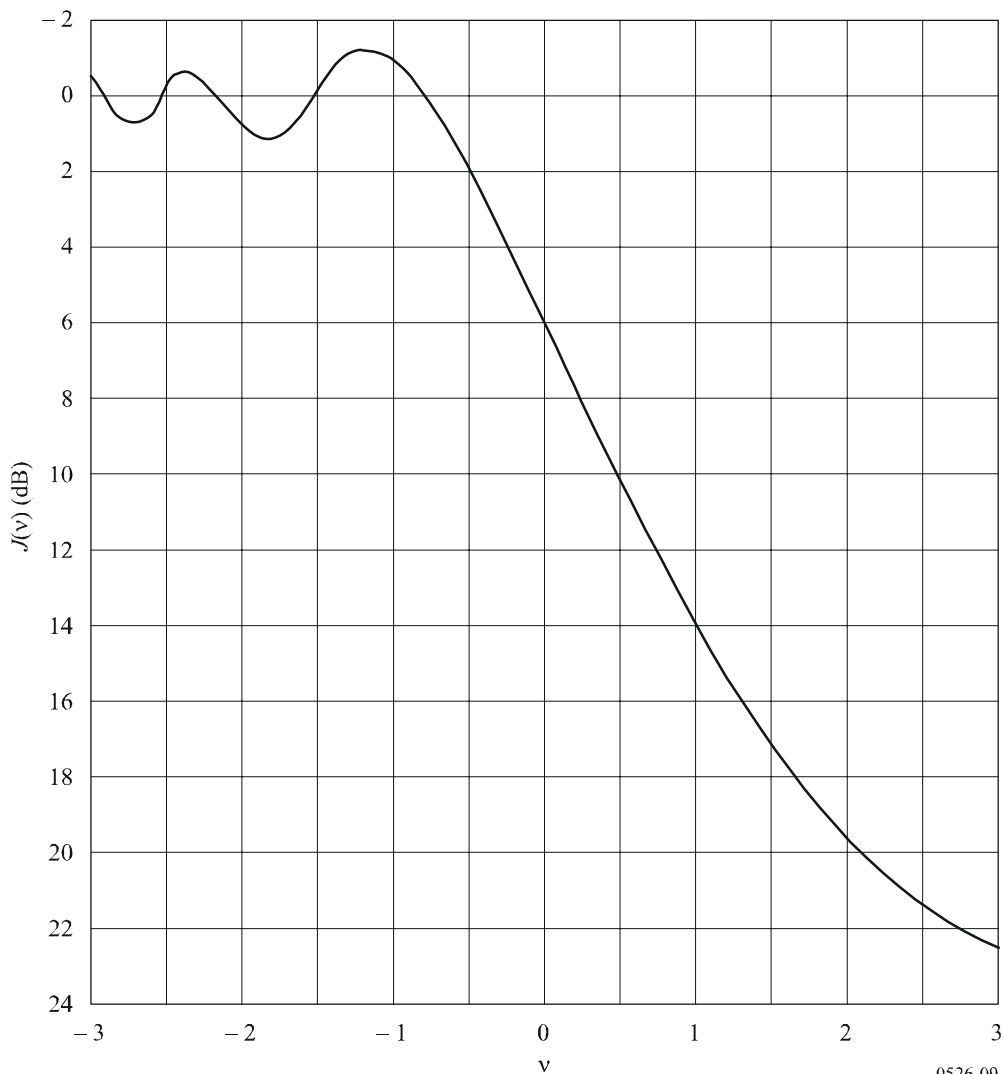
$$J(v) = -20 \log \left(\frac{\sqrt{[1 - C(v) - S(v)]^2 + [C(v) - S(v)]^2}}{2} \right) \quad (26)$$

where $C(v)$ and $S(v)$ are the real and imaginary parts respectively of the complex Fresnel integral $F(v)$ defined in § 2.7.

For v greater than -0.78 an approximate value can be obtained from the expression:

$$J(v) = 6.9 + 20 \log \left(\sqrt{(v - 0.1)^2 + 1} + v - 0.1 \right) \quad \text{dB} \quad (27)$$

FIGURE 9
Knife-edge diffraction loss



4.2 Single rounded obstacle

The geometry of a rounded obstacle of radius R is illustrated in Fig. 8c). Note that the distances d_1 and d_2 , and the height h above the baseline, are all measured to the vertex where the projected rays intersect above the obstacle. The diffraction loss for this geometry may be calculated as:

$$A = J(v) + T(m,n) \quad \text{dB} \quad (28)$$

where:

- a) $J(v)$ is the Fresnel-Kirchoff loss due to an equivalent knife-edge placed with its peak at the vertex point. The dimensionless parameter v may be evaluated from any of equations (22) to (25) inclusive. For example, in practical units equation (22) may be written:

$$v = 0.0316h \left[\frac{2(d_1 + d_2)}{\lambda d_1 d_2} \right]^{1/2} \quad (29)$$

where h and λ are in metres, and d_1 and d_2 are in kilometres.

$J(v)$ may be obtained from Fig. 9 or from equation (27). Note that for an obstruction to LoS propagation, v is positive and equation (27) is valid.

- b) $T(m,n)$ is the additional attenuation due to the curvature of the obstacle:

$$T(m,n) = 7.2m^{1/2} - (2 - 12.5n)m + 3.6m^{3/2} - 0.8m^2 \quad \text{dB} \quad \text{for } mn \leq 4 \quad (30a)$$

$$T(m,n) = -6 - 20 \log(mn) + 7.2m^{1/2} - (2 - 17n)m + 3.6m^{3/2} - 0.8m^2 \quad \text{dB} \quad \text{for } mn > 4 \quad (30b)$$

and

$$m = R \left[\frac{d_1 + d_2}{d_1 d_2} \right] \left/ \left[\frac{\pi R}{\lambda} \right]^{1/3} \right. \quad (31)$$

$$n = h \left[\frac{\pi R}{\lambda} \right]^{2/3} \left/ R \right. \quad (32)$$

and R , d_1 , d_2 , h and λ are in self-consistent units.

Note that as R tends to zero, $T(m,n)$ also tend to zero. Thus equation (28) reduces to knife-edge diffraction for a cylinder of zero radius.

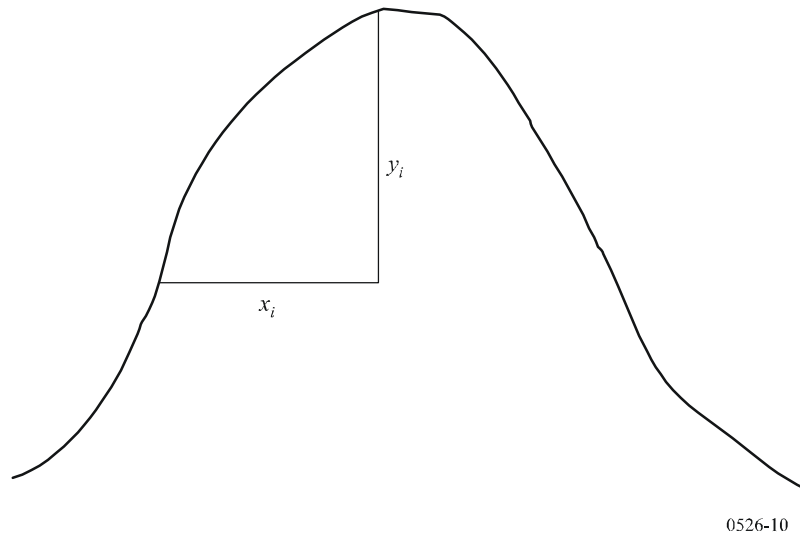
The obstacle radius of curvature corresponds to the radius of curvature at the apex of a parabola fitted to the obstacle profile in the vicinity of the top. When fitting the parabola, the maximum vertical distance from the apex to be used in this procedure should be of the order of the first Fresnel zone radius where the obstacle is located. An example of this procedure is shown in Fig. 10, where:

$$y_i = \frac{x_i^2}{2r_i} \quad (33)$$

and r_i is the radius of curvature corresponding to the sample i of the vertical profile of the ridge. In the case of N samples, the median radius of curvature of the obstacle is given by:

$$r = \frac{1}{N} \sum_1^N \frac{x_i^2}{2y_i} \quad (34)$$

FIGURE 10
Vertical profile of the obstacle



4.3 Double isolated edges

This method consists of applying single knife-edge diffraction theory successively to the two obstacles, with the top of the first obstacle acting as a source for diffraction over the second obstacle (see Fig. 11). The first diffraction path, defined by the distances a and b and the height h'_1 , gives a loss L_1 (dB). The second diffraction path, defined by the distances b and c and the height h'_2 , gives a loss L_2 (dB). L_1 and L_2 are calculated using formulae of § 4.1. A correction term L_c (dB) must be added to take into account the separation b between the edges. L_c may be estimated by the following formula:

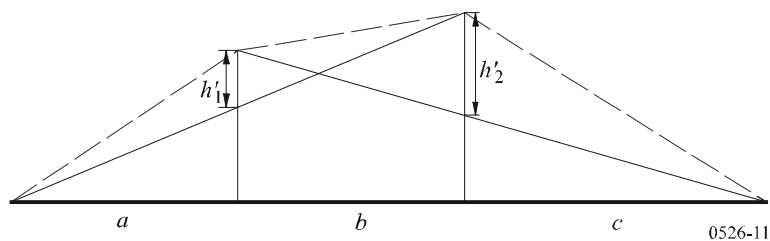
$$L_c = 10 \log \left[\frac{(a + b)(b + c)}{b(a + b + c)} \right] \quad (35)$$

which is valid when each of L_1 and L_2 exceeds about 15 dB. The total diffraction loss is then given by:

$$L = L_1 + L_2 + L_c \quad (36)$$

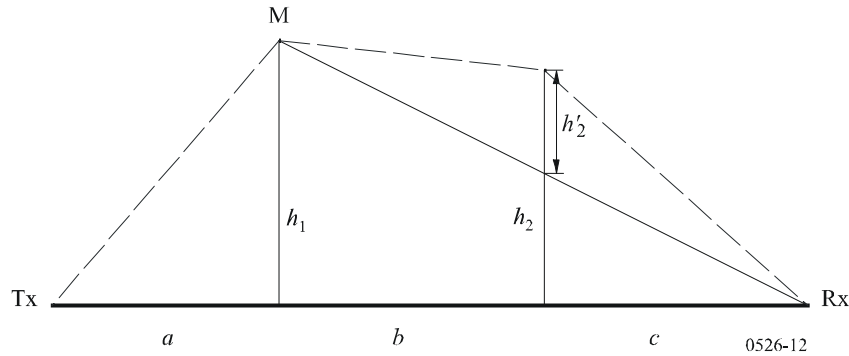
The above method is particularly useful when the two edges give similar losses.

FIGURE 11
Method for double isolated edges



If one edge is predominant (see Fig. 12), the first diffraction path is defined by the distances a and $b + c$ and the height h_1 . The second diffraction path is defined by the distances b and c and the height h'_2 .

FIGURE 12
Figure showing the main and the second obstacle



The method consists of applying single knife-edge diffraction theory successively to the two obstacles. First, the higher h/r ratio determines the main obstacle, M, where h is the edge height from the direct path $TxRx$ as shown in Fig. 12, and r is the first Fresnel ellipsoid radius given by equation (2). Then h'_2 , the height of the secondary obstacle from the sub-path MR, is used to calculate the loss caused by this secondary obstacle. A correction term T_c (dB) must be subtracted, in order to take into account the separation between the two edges as well as their height. T_c (dB) may be estimated by the following formula:

$$T_c = \left[12 - 20 \log_{10} \left(\frac{2}{1 - \frac{a}{\pi}} \right) \right] \left(\frac{q}{p} \right)^{2p} \quad (37)$$

with:

$$p = \left[\frac{2(a+b+c)}{\lambda(b+c)a} \right]^{1/2} h_1 \quad q = \left[\frac{2(a+b+c)}{\lambda(a+b)c} \right]^{1/2} h_2 \quad \tan \alpha = \left[\frac{b(a+b+c)}{ac} \right]^{1/2} \quad (38)$$

h_1 and h_2 are the edge heights from the direct path transmitter-receiver.

The total diffraction loss is given by:

$$L = L_1 + L_2 - T_c \quad (39)$$

The same method may be applied to the case of rounded obstacles using § 4.3.

In cases where the diffracting obstacle may be clearly identified as a flat-roofed building a single knife-edge approximation is not sufficient. It is necessary to calculate the phasor sum of two components: one undergoing a double knife-edge diffraction and the other subject to an additional reflection from the roof surface. It has been shown that, where the reflectivity of the roof surface and any difference in height between the roof surface and the side walls are not accurately known, then a double knife-edge model produces a good prediction of the diffracted field strength, ignoring the reflected component.

4.4 Multiple isolated obstacles

Two methods are recommended for the diffraction over irregular terrain which forms one or more obstacles to LoS propagation. The first method assumes that each obstacle can be represented by a cylinder with a radius equal to the radius of curvature at the obstacle top, being advisable when detailed vertical profile through the ridge is available.

The second one corresponds to an empirical solution based on the supposition of knife-edge obstacles plus a correction to compensate for the higher loss due to a radius of curvature different from zero. The calculation takes Earth curvature into account via the concept of an effective Earth radius (see Recommendation ITU-R P.452, § 4.3). This method is suitable in cases where a single general procedure is required for terrestrial paths over land or sea and for both LoS and transhorizon.

A profile of the radio path should be available consisting of a set of samples of ground height above sea level ordered at intervals along the path, the first and last being the heights of the transmitter and receiver above sea level, and a corresponding set of horizontal distances from the transmitter. Each height and distance pair are referred to as a profile point and given an index, with indices incrementing from one end of the path to the other. Although it is not essential to the method, in the following description it is assumed that indices increment from the transmitter to the receiver. It is preferable but not essential for the profile samples to be equally spaced horizontally.

4.4.1 Cascaded cylinder method

The terrain height profile should be available as a set of samples of ground height above sea level, the first and last being the heights of the transmitter and receiver above sea level. Distance and height values are described as though stored in arrays indexed from 1 to N , where N equals the number of profile samples.

In the following a systematic use of suffices is made:

h_i : height above sea level of the i -th point

d_i : distance from the transmitter to the i -th point

d_{ij} : distance from the i -th to the j -th points.

The first step is to perform a “stretched string” analysis of the profile. This identifies the sample points which would be touched by a string stretched over the profile from transmitter to receiver. This may be done by the following procedure, in which all values of height and distance are in self-consistent units, and all angles are in radians. The method includes approximations which are valid for radio paths making small angles to the horizontal. If a path has ray gradients exceeding about 5° more exact geometry may be justified.

Each string point is identified as the profile point with the highest angular elevation above the local horizontal as viewed from the previous string point, starting at one end of the profile and finishing at the other. Viewed from point s , the elevation of the i -th profile sample ($i > s$) is given by:

$$e = [(h_i - h_s) / d_{si}] - [d_{si} / 2a_e] \quad (40)$$

where:

a_e : effective Earth radius, given by:
 $= k \times 6371$ (km)

and

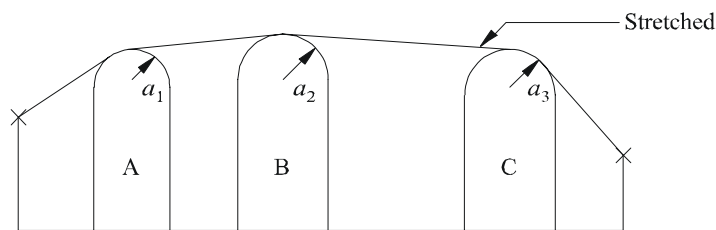
k : effective Earth-radius factor.

A test is now applied to determine whether any group of two or more string points should represent the same terrain obstruction. For samples at spacings of 250 m or less any group of string points which are consecutive profile samples, other than the transmitter or receiver, should be treated as one obstruction.

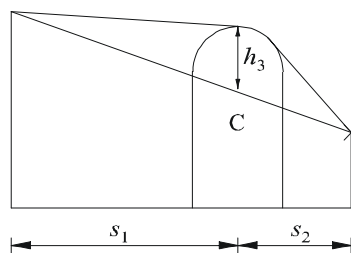
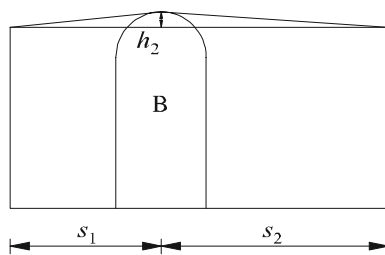
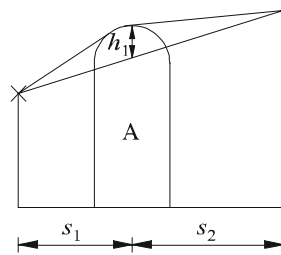
Each obstruction is now modelled as a cylinder, as illustrated in Fig. 13. The geometry of each individual cylinder corresponds with Fig. 8c). Note that in Fig. 13 the distances s_1, s_2 for each cylinder are shown as measured horizontally between the vertex points, and that for near-horizontal rays these distances approximate to the slope distances d_1 and d_2 in Fig. 8c). For ray angles to the horizontal greater than about 5° it may be necessary to set s_1 and s_2 to the inter-vertex slope distances d_1 and d_2 .

FIGURE 13

The cascaded cylinder model a), overall problem b), details



a)



b)

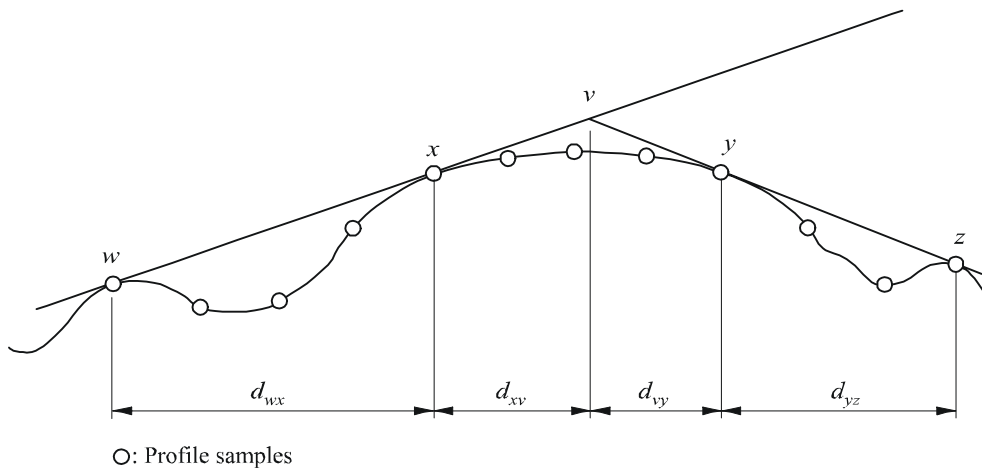
0526-13
)

Similarly in Fig. 13, the height h of each cylinder is shown as measured vertically from its vertex down to the straight line joining the adjacent vertex or terminal points. The value of h for each cylinder corresponds to h in Fig. 8c). Again, for near-horizontal rays the cylinder heights may be computed as though vertical, but for steeper ray angles it may be necessary to compute h at right angles to the baseline of its cylinder.

Figure 14 illustrates the geometry for an obstruction consisting of more than one string point. The following points are indicated by:

- w : closest string point or terminal on the transmitter side of the obstruction which is not part of the obstruction
- x : string point forming part of the obstruction which is closest to the transmitter
- y : string point forming part of the obstruction which is closest to the receiver
- z : closest string point or terminal on the receiver side of the obstruction which is not part of the obstruction
- v : vertex point made by the intersection of incident rays above the obstruction.

FIGURE 14
Geometry of a multipoint obstacle



0526-14

The letters w , x , y and z will also be indices to the arrays of profile distance and height samples. For an obstruction consisting of an isolated string point, x and y will have the same value, and will refer to a profile point which coincides with the vertex. Note that for cascaded cylinders, points y and z for one cylinder are points w and x for the next, etc.

A step-by-step method for fitting cylinders to a general terrain profile is described in Appendix 1 to Annex 1. Each obstruction is characterized by w , x , y and z . The method of Appendix 1 to Annex 1 is then used to obtain the cylinder parameters s_1 , s_2 , h and R . Having modelled the profile in this way, the diffraction loss for the path is computed as the sum of three terms:

- the sum of diffraction losses over the cylinders;
- the sum of sub-path diffraction between cylinders (and between cylinders and adjacent terminals);
- a correction term.

The total diffraction loss, in dB relative to free-space loss, may be written:

$$L_d = \sum_{i=1}^N L'_i + L''(wx)_1 + \sum_{i=1}^N L''(yz)_i - 20 \log C_N \quad \text{dB} \quad (41)$$

where:

- L'_i : diffraction loss over the i -th cylinder calculated by the method of § 4.2
- $L''(wx)_1$: sub-path diffraction loss for the section of the path between points w and x for the first cylinder
- $L''(yz)_i$: sub-path diffraction loss for the section of the path between points y and z for all cylinders
- C_N : correction factor to account for spreading loss due to diffraction over successive cylinders.

Appendix 2 to Annex 1 gives a method for calculating L'' for each LoS section of the path between obstructions.

The correction factor, C_N , is calculated using:

$$C_N = (P_a / P_b)^{0.5} \quad (42)$$

where:

$$P_a = s_1 \prod_{i=1}^N [(s_2)_i] \left(s_1 + j \sum_{j=1}^N [(s_2)_j] \right) \quad (43)$$

$$P_b = (s_1)_1 (s_2)_N \prod_{i=1}^N [(s_1)_i + (s_2)_i] \quad (44)$$

and the suffices to round brackets indicate individual cylinders.

4.4.2 Cascaded knife edge method

The method is based on a procedure which is used from 1 to 3 times depending on the path profile. The procedure consists of finding the point within a given section of the profile with the highest value of the geometrical parameter v as described in § 4.1. The section of the profile to be considered is defined from point index a to point index b ($a < b$). If $a + 1 = b$ there is no intermediate point and the diffraction loss for the section of the path being considered is zero. Otherwise the construction is applied by evaluating v_n ($a < n < b$) and selecting the point with the highest value of v . The value of v for the n -th profile point is given by:

$$v_n = h \sqrt{2d_{ab} / \lambda d_{an} d_{nb}} \quad (45)$$

where:

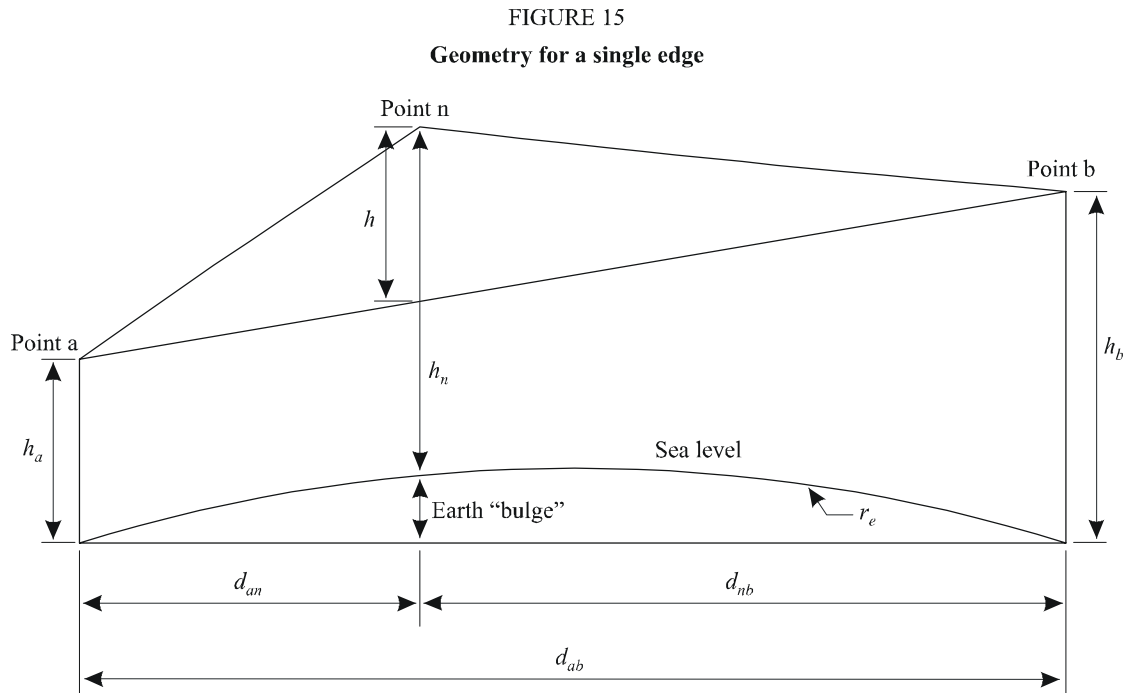
$$h = h_n + [d_{an} d_{nb} / 2 r_e] - [(h_a d_{nb} + h_b d_{an}) / d_{ab}] \quad (45a)$$

- h_a, h_b, h_n : vertical heights as shown in Fig. 15
- d_{an}, d_{nb}, d_{ab} : horizontal distances as shown in Fig. 15
- r_e : effective Earth radius
- λ : wavelength

and all h, d, r_e and λ are in self-consistent units.

The diffraction loss is then given as the knife-edge loss $J(v)$ according to equation (27) for $v > -0.78$, and is otherwise zero.

Note that equation (45) is derived directly from equation (22). The geometry of equation (45a) is illustrated in Fig. 15. The second term in equation (45a) is a good approximation to the additional height at point n due to Earth curvature.



0526-15

The above procedure is first applied to the entire profile from transmitter to receiver. The point with the highest value of v is termed the principal edge, p , and the corresponding loss is $J(v_p)$.

If $v_p > -0.78$ the procedure is applied twice more:

- from the transmitter to point p to obtain v_t and hence $J(v_t)$;
- from point p to the receiver to obtain v_r and hence $J(v_r)$.

The excess diffraction loss for the path is then given by:

$$L = J(v_p) + T [J(v_t) + J(v_r) + C] \quad \text{for } v_p > -0.78 \quad (46a)$$

$$L = 0 \quad \text{for } v_p \leq -0.78 \quad (46b)$$

where:

C : empirical correction

$$C = 10.0 + 0.04D \quad (47)$$

D : total path length (km)

and

$$T = 1.0 - \exp [-J(v_p)/6.0] \quad (48)$$

Note that the above procedure, for transhorizon paths, is based on the Deygout method limited to a maximum of 3 edges. For line-of-sight paths it differs from the Deygout construction in that two secondary edges are still used in cases where the principal edge results in a non-zero diffraction loss.

Where this method is used to predict diffraction loss for different values of effective Earth radius over the same path profile, it is recommended that the principal edge, and if they exist the auxiliary edges on either side, are first found for median effective Earth radius. These edges should then be used when calculating diffraction losses for other values of effective Earth radius, without repeating the procedure for locating these points. This avoids the possibility, which may occur in a few cases, of a discontinuity in predicted diffraction loss as a function of effective Earth radius due to different edges being selected.

5 Diffraction by thin screens

The following methods assume that the obstruction is in the form of a thin screen. They can be applied to propagation around an obstacle or through an aperture.

5.1 Finite-width screen

Interference suppression for a receiving site (e.g. a small earth station) may be obtained by an artificial screen of finite width transverse to the direction of propagation. For this case the field in the shadow of the screen may be calculated by considering three knife-edges, i.e. the top and the two sides of the screen. Constructive and destructive interference of the three independent contributions will result in rapid fluctuations of the field strength over distances of the order of a wavelength. The following simplified model provides estimates for the average and minimum diffraction loss as a function of location. It consists of adding the amplitudes of the individual contributions for an estimate of the minimum diffraction loss and a power addition to obtain an estimate of the average diffraction loss. The model has been tested against accurate calculations using the uniform theory of diffraction (UTD) and high-precision measurements.

Step 1: Calculate the geometrical parameter v for each of the three knife-edges (top, left side and right side) using any of equations (22) to (25).

Step 2: Calculate the loss factor $j(v) = 10^{J(v)/20}$ associated with each edge from equation (27).

Step 3: Calculate minimum diffraction loss J_{min} from:

$$J_{min}(v) = -20 \log \left[\frac{1}{j_1(v)} + \frac{1}{j_2(v)} + \frac{1}{j_3(v)} \right] \quad \text{dB} \quad (49)$$

or, alternatively,

Step 4: Calculate average diffraction loss J_{av} from:

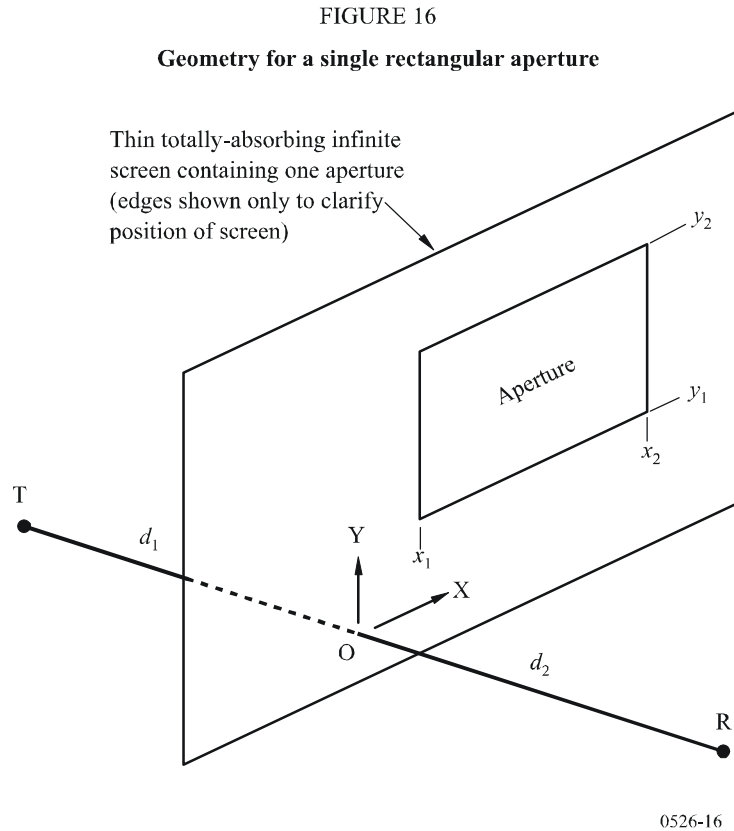
$$J_{av}(v) = -10 \log \left[\frac{1}{j_1^2(v)} + \frac{1}{j_2^2(v)} + \frac{1}{j_3^2(v)} \right] \quad \text{dB} \quad (50)$$

5.2 Diffraction by rectangular apertures and composite apertures or screens

The method described below can be used to predict the diffraction loss due to a rectangular aperture in an otherwise totally-absorbing thin screen. The method can be extended to cover several rectangular apertures or finite screens, and is thus an alternative method for the finite-width screen discussed in § 5.1.

5.2.1 Diffraction by a single rectangular aperture

Figure 16 shows the geometry used to represent a rectangular aperture in an infinite totally-absorbing thin screen.



The positions of the aperture edges, x_1 , x_2 , y_1 and y_2 , are given in a Cartesian coordinate system with origin at the point where the straight line from transmitter T to receiver R passes through the screen, with propagation parallel to the Z axis. T and R are at distances d_1 and d_2 respectively behind and in front of the screen.

The field strength, e_a , at the receiver in linear units normalized to free space is given in complex form by:

$$e_a(x_1, x_2, y_1, y_2) = 0.5(C_x C_y - S_x S_y) + j 0.5 (C_x S_y + S_x C_y) \quad (51)$$

where:

$$C_x = C(v_{x2}) - C(v_{x1}) \quad (52a)$$

$$C_y = C(v_{y2}) - C(v_{y1}) \quad (52b)$$

$$S_x = S(v_{x2}) - S(v_{x1}) \quad (52c)$$

$$S_y = S(v_{y2}) - S(v_{y1}) \quad (52d)$$

The four values of v are as given by equation (22) substituting x_1 , x_2 , y_1 and y_2 in turn for h , and $C(v)$ and $S(v)$ are as given in equations (7a) and (7b) and may be evaluated from the complex Fresnel coefficient using equations (8a) and (8b).

The corresponding diffraction loss L_a is given by:

$$L_a = -20 \log(e_a) \quad \text{dB} \quad (53)$$

5.2.2 Diffraction by composite apertures or screens

The method for a single rectangular aperture can be extended as follows:

Since in the linear units normalized to free space of equation (51) the free-space field is given by $1.0 + j 0.0$, the normalized complex field e_s due to a single rectangular screen (isolated from ground) is given by:

$$e_s = 1.0 - e_a \tag{54}$$

where e_a is calculated using equation (51) for an aperture of the same size and position as the screen.

- The normalized field due to combinations of several rectangular apertures or isolated screens can be calculated by adding the results of equation (51) or (54).
- Arbitrarily shaped apertures or screens can be approximated by suitable combinations of rectangular apertures or screens.
- Since the $C(v)$ and $S(v)$ integrals converge to $0.5 + j 0.5$ as v approaches infinity, equation (50) can be applied to rectangles of unlimited extent in one or more directions.

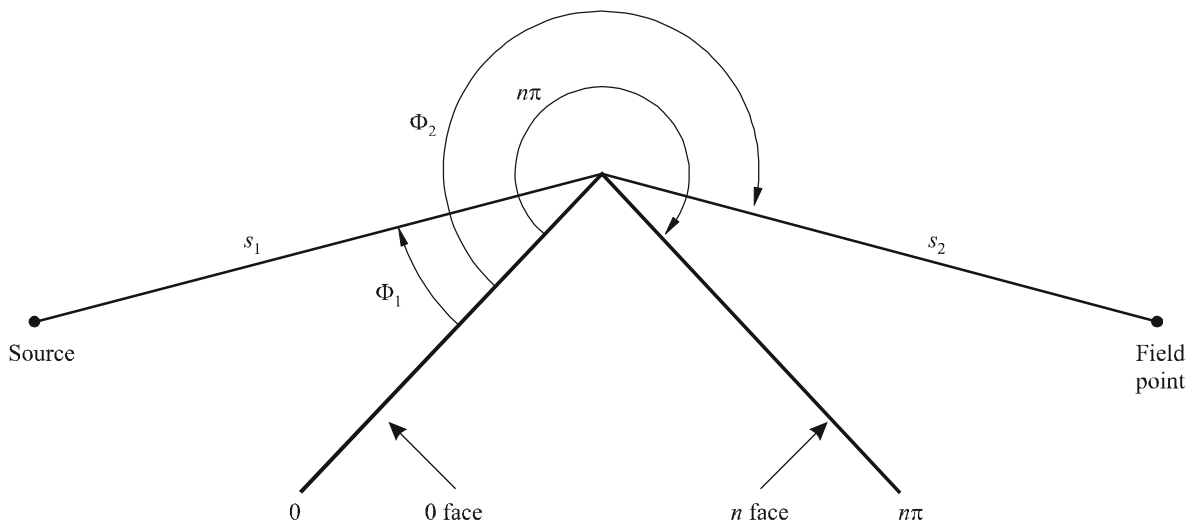
6 Diffraction over a finitely conducting wedge

The method described below can be used to predict the diffraction loss due to a finitely conducting wedge. Suitable applications are for diffraction around the corner of a building or over the ridge of a roof, or where terrain can be characterized by a wedge-shaped hill. The method requires the conductivity and relative dielectric constant of the obstructing wedge, and assumes that no transmission occurs through the wedge material.

The method is based on UTD. It takes account of diffraction in both the shadow and line-of-sight region, and a method is provided for a smooth transition between these regions.

The geometry of a finitely conducting wedge-shaped obstacle is illustrated in Fig. 17.

FIGURE 17
Geometry for application of UTD wedge diffraction



The UTD formulation for the electric field at the field point, specializing to two dimensions, is:

$$e_{UTD} = e_0 \frac{\exp(-jks_1)}{s_1} D_{\parallel}^{\dagger} \cdot \sqrt{\frac{s_1}{s_2(s_1 + s_2)}} \cdot \exp(-jks_2) \quad (55)$$

where:

- e_{UTD} : electric field at the field point
- e_0 : relative source amplitude
- s_1 : distance from source point to diffracting edge
- s_2 : distance from diffracting edge to field point
- k : wave number $2\pi/\lambda$
- D_{\parallel}^{\dagger} : diffraction coefficient depending on the polarization (parallel or perpendicular to the plane of incidence) of the incident field on the edge

and s_1 , s_2 and λ are in self-consistent units.

The diffraction coefficient for a finitely conducting wedge is given as:

$$D_{\parallel}^{\dagger} = \frac{-\exp(-j\pi/4)}{2n\sqrt{2\pi k}} \left\{ \begin{array}{l} \cot\left(\frac{\pi + (\Phi_2 - \Phi_1)}{2n}\right) \cdot F(kLa^+(\Phi_2 - \Phi_1)) \\ + \cot\left(\frac{\pi - (\Phi_2 - \Phi_1)}{2n}\right) \cdot F(kLa^-(\Phi_2 - \Phi_1)) \\ + R_0^{\dagger} \cdot \cot\left(\frac{\pi - (\Phi_2 + \Phi_1)}{2n}\right) \cdot F(kLa^-(\Phi_2 + \Phi_1)) \\ + R_n^{\dagger} \cdot \cot\left(\frac{\pi + (\Phi_2 + \Phi_1)}{2n}\right) \cdot F(kLa^+(\Phi_2 + \Phi_1)) \end{array} \right\} \quad (56)$$

where:

- Φ_1 : incidence angle, measured from incidence face (0 face)
- Φ_2 : diffraction angle, measured from incidence face (0 face)
- n : external wedge angle as a multiple of π radians (actual angle = $n\pi$ (rad))
- $j = \sqrt{-1}$

and where $F(x)$ is a Fresnel integral:

$$F(x) = 2j\sqrt{x} \cdot \exp(jx) \cdot \int_{\sqrt{x}}^{\infty} \exp(-jt^2) dt \quad (57)$$

$$\int_{\sqrt{x}}^{\infty} \exp(-jt^2) dt = \sqrt{\frac{\pi}{8}}(1 - j) - \int_0^{\sqrt{x}} \exp(-jt^2) dt \quad (58)$$

The integral may be calculated by numerical integration.

Alternatively a useful approximation is given by:

$$\int_{\sqrt{x}}^{\infty} \exp(-jt^2) dt = \sqrt{\frac{\pi}{2}} A(x) \quad (59)$$

where:

$$A(x) = \left\{ \begin{array}{ll} \frac{1-j}{2} - \exp(-jx) \sqrt{\frac{x}{4}} \sum_{n=0}^{11} \left[(a_n + jb_n) \left(\frac{x}{4}\right)^n \right] & \text{if } x < 4 \\ -\exp(-jx) \sqrt{\frac{4}{x}} \sum_{n=0}^{11} \left[(c_n + jd_n) \left(\frac{4}{x}\right)^n \right] & \text{otherwise} \end{array} \right\} \quad (60)$$

and the coefficients a, b, c, d are given in § 2.7.

$$L = \frac{s_2 \cdot s_1}{s_2 + s_1} \quad (61)$$

$$a^\pm(\beta) = 2 \cos^2 \left(\frac{2n\pi N^\pm - \beta}{2} \right) \quad (62)$$

where:

$$\beta = \Phi_2 \pm \Phi_1 \quad (63)$$

In equation (41), N^\pm are the integers which most nearly satisfy the equation.

$$N^\pm = \frac{\beta \pm \pi}{2n\pi} \quad (64)$$

R_0^\perp, R_n^\perp are the reflection coefficients for either perpendicular or parallel polarization given by:

$$R^\perp = \frac{\sin(\Phi) - \sqrt{\eta - \cos(\Phi)^2}}{\sin(\Phi) + \sqrt{\eta - \cos(\Phi)^2}} \quad (65)$$

$$R^\parallel = \frac{\eta \cdot \sin(\Phi) - \sqrt{\eta - \cos(\Phi)^2}}{\eta \cdot \sin(\Phi) + \sqrt{\eta - \cos(\Phi)^2}} \quad (66)$$

where:

$$\Phi = \Phi_1 \text{ for } R_0 \text{ and } \Phi = (n\pi - \Phi_2) \text{ for } R_n$$

$$\eta = \epsilon_r - j \times 18 \times 10^9 \sigma / f$$

ϵ_r : relative dielectric constant of the wedge material

σ : conductivity of the wedge material (S/m)

f : frequency (Hz).

Note that if necessary the two faces of the wedge may have different electrical properties.

At shadow and reflection boundaries one of the cotangent functions in equation (56) becomes singular.

However D^{\perp} remains finite, and can be readily evaluated. The term containing the singular cotangent function is given for small ε as:

$$\cot\left(\frac{\pi \pm \beta}{2n}\right) \cdot F(kLa^{\pm}(\beta)) \cong n \cdot \left[\sqrt{2\pi kL} \cdot \text{sign}(\varepsilon) - 2kL\varepsilon \cdot \exp(j\pi/4)\right] \cdot \exp(j\pi/4) \quad (67)$$

with ε defined by:

$$\varepsilon = \pi + \beta - 2\pi nN^+ \quad \text{for} \quad \beta = \Phi_2 + \Phi_1 \quad (68)$$

$$\varepsilon = \pi - \beta + 2\pi nN^- \quad \text{for} \quad \beta = \Phi_2 - \Phi_1 \quad (69)$$

The resulting diffraction coefficient will be continuous at shadow and reflection boundaries, provided that the same reflection coefficient is used when calculating reflected rays.

The field e_{LD} due to the diffracted ray, plus the LoS ray for $(\Phi_2 - \Phi_1) < \pi$, is given by:

$$e_{LD} = \begin{cases} e_{UTD} + \frac{\exp(-jks)}{s} & \text{for} \quad \Phi_2 < \Phi_1 + \pi \\ e_{UTD} & \text{for} \quad \Phi_2 \geq \Phi_1 + \pi \end{cases} \quad (70)$$

where:

s : straight-line distance between the source and field points.

Note that at $(\Phi_2 - \Phi_1) = \pi$ the 2nd cotangent term in equation (56) will become singular, and that the alternative approximation given by equation (67) must be used.

The field strength at the field point (dB) relative to the field which would exist at the field point in the absence of the wedge-shaped obstruction (i.e. dB relative to free space) is given by setting e_0 to unity in equation (55) and calculating:

$$E_{UTD} = 20 \log\left(\left|\frac{s \cdot e_{UTD}}{\exp(-jks)}\right|\right) \quad (71)$$

where:

s : straight-line distance between the source and field points.

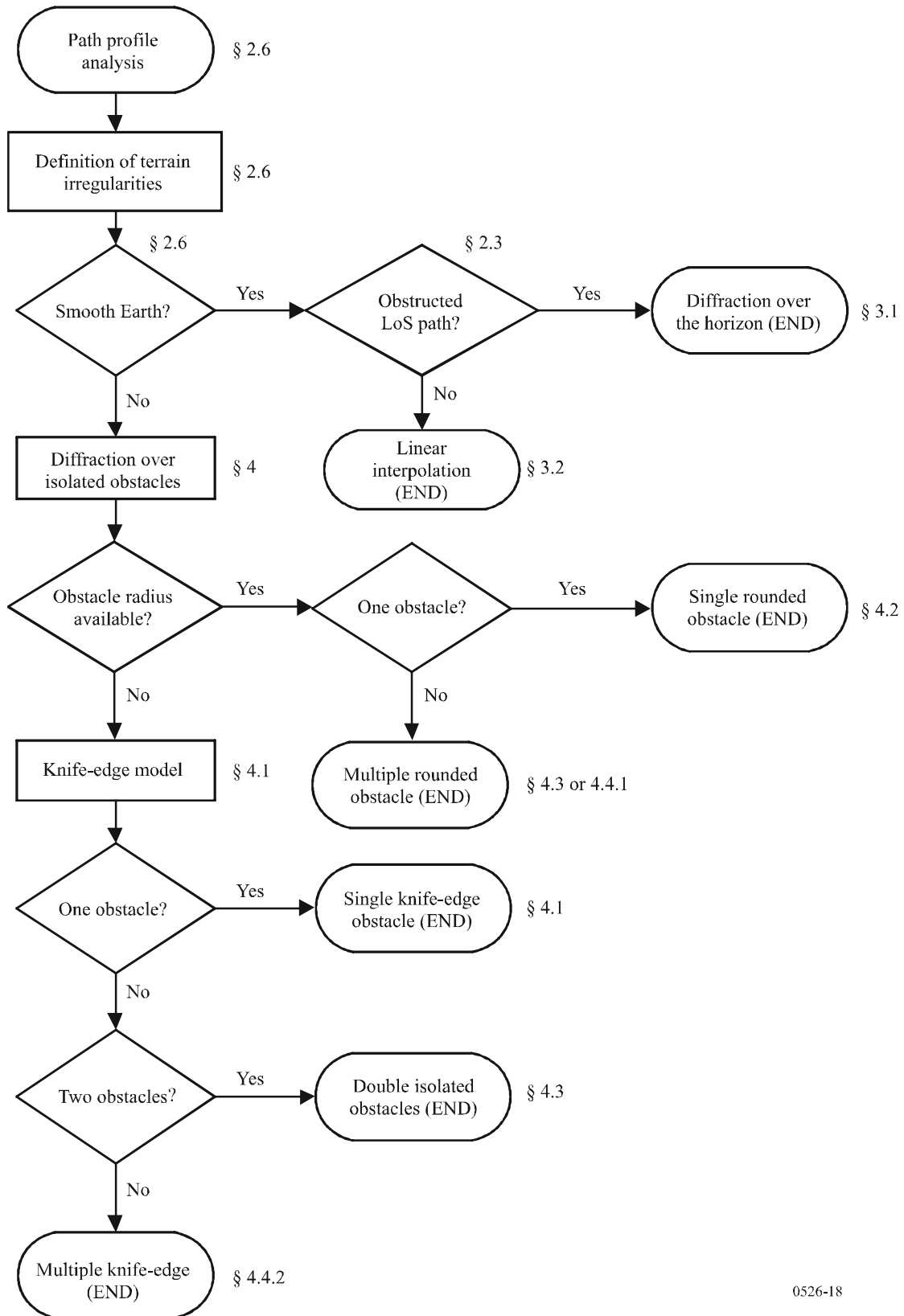
Note that, for $n = 2$ and zero reflection coefficients, this should give the same results as the knife edge diffraction loss curve shown in Fig. 9.

A MathCAD version of the UTD formulation is available from the Radiocommunication Bureau.

7 Guide to propagation by diffraction

A general guide for the evaluation of diffraction loss corresponding to § 3 and 4 is shown in Fig. 18. This flow chart summarizes the procedure to be adopted in each case.

FIGURE 18
Guide to propagation by diffraction



Appendix 1 to Annex 1

Calculation of cylinder parameters

The following procedure can be used to calculate the cylinder parameters illustrated in Figs. 8c) and 14 for each of the terrain obstructions. Self-consistent units are used, and all angles are in radians. The approximations used are valid for radio paths which are within about 5° of horizontal.

1 Diffraction angle and position of vertex

Although not used directly as cylinder parameters, both the diffraction angle over the cylinder and the position of the vertex are required.

The diffraction angle over the obstacle is given by:

$$\theta = \alpha_w + \alpha_z + \alpha_e \quad (72)$$

where α_w and α_z are the angular elevations of points x and y above the local horizontal as viewed from points w and z respectively, given by:

$$\alpha_w = (h_x - h_w) / d_{wx} - d_{wx} / 2a_e \quad (73)$$

$$\alpha_z = (h_y - h_z) / d_{yz} - d_{yz} / 2a_e \quad (74)$$

and α_e is the angle subtended by the great-circle distance between points w and z given by:

$$\alpha_e = d_{wz} / a_e \quad (75)$$

The distance of the vertex from point w is calculated according to whether the obstruction is represented by a single profile sample or by more than one:

For a single-point obstruction:

$$d_{wv} = d_{wx} \quad (76)$$

For a multipoint obstruction it is necessary to protect against very small values of diffraction:

$$d_{wv} = [(\alpha_z + \alpha_e / 2) d_{wz} + h_z - h_w] / \theta \quad \text{for } \theta \cdot a_e \geq d_{xy} \quad (77a)$$

$$d_{wv} = (d_x + d_y) / 2 \quad \text{for } \theta \cdot a_e < d_{xy} \quad (77b)$$

The distance of point z from the vertex point is given by:

$$d_{vz} = d_{wz} - d_{wv} \quad (78)$$

The height of the vertex point above sea level is calculated according to whether the obstruction is represented by a single profile sample or by more than one.

For a single point obstruction:

$$h_v = h_x \quad (79)$$

For a multipoint obstruction:

$$h_v = d_{wv} \alpha_w + h_w + d_{2,wv} / 2a_e \quad (80)$$

2 Cylinder parameters

The cylinder parameters illustrated in Fig. 8c) can now be calculated for each of the terrain obstacles defined by the string analysis:

d_1 and d_2 are the positive inter-vertex distances to the obstacles (or terminals) on the transmitter and receiver sides of the obstacle respectively,

and:

$$h = h_v + d_{wv} d_{vz} / 2a_e - (h_w d_{vz} + h_z d_{wv}) / d_{wz} \quad (81)$$

To calculate the cylinder radius use is made of two further profile samples:

p : the point adjacent to x on the transmitter side,

and:

q : the point adjacent to y on the receiver side

Thus the profile indices p and q are given by:

$$p = x - 1 \quad (82)$$

and:

$$q = y + 1 \quad (83)$$

If a point given by p or q is a terminal, then the corresponding value of h should be the terrain height at that point, not the height above sea level of the antenna.

The cylinder radius is calculated as the difference in slope between the profile section p - x and y - q , allowing for Earth curvature, divided by the distance between p and q .

The distances between profile samples needed for this calculation are:

$$d_{px} = d_x - d_p \quad (84)$$

$$d_{yq} = d_q - d_y \quad (85)$$

$$d_{pq} = d_q - d_p \quad (86)$$

The difference in slope between the p - x and y - q profile sections is given in radians by:

$$t = (h_x - h_p) / d_{px} + (h_y - h_q) / d_{yq} - d_{pq} / a_e \quad (87)$$

where a_e is the effective Earth radius.

The cylinder radius is now given by:

$$R = [d_{pq} / t] [1 - \exp(4v)]^3 \quad (88)$$

where v is the dimensionless knife-edge parameter in equation (28).

In equation (48), the second factor is an empirical smoothing function applied to the cylinder radius to avoid discontinuities for marginally LoS obstructions.

Appendix 2 to Annex 1

Sub-path diffraction losses

1 Introduction

This Appendix provides a method for computing the sub-path diffraction loss for a LoS subsection of a diffraction path. The path has been modelled by cascaded cylinders each characterized by profile points w , x , y and z as illustrated in Figs. 13 and 14. The sub-path diffraction is to be calculated for each subsection of the overall path between points represented by w and x , or by y and z . These are the LoS sections of the path between obstructions, or between a terminal and an obstruction.

The method can also be used for a LoS with sub-path diffraction, in which case it is applied to the entire path.

2 Method

For a LoS section of the profile between profile samples indexed by u and v , the first task is to identify the profile sample between but excluding u and v which obstructs the largest fraction of the first Fresnel zone for a ray travelling from u to v .

To avoid selecting a point which is essentially part of one of the terrain obstacles already modelled as a cylinder, the profile between u and v is restricted to a section between two additional indices p and q , which are set as follows:

- Set $p = u + 1$.
- If both $p < v$ and $h_p > h_{p+1}$, then increase p by 1 and repeat.
- Set $q = v - 1$.
- If both $q > u$ and $h_q > h_{q-1}$, then decrease q by 1 and repeat.

If $p = q$ then the sub-path obstruction loss is set to 0. Otherwise the calculation proceeds as follows.

It is now necessary to find the minimum value of normalized clearance, C_F , given by h_z/F_1 , where in self-consistent units:

h_z : height of ray above profile point

F_1 : radius of first Fresnel zone.

The minimum normalized clearance may be written:

$$C_F = \min_{i=p}^q [(h_z)_i / (F_1)_i] \quad (89)$$

where:

$$(h_z)_i = (h_r)_i - (h_t)_i \quad (90)$$

$$(F_1)_i = \sqrt{\lambda \cdot d_{ui} \cdot d_{iv} / d_{uv}} \quad (91)$$

$(h_r)_i$, the height of the ray above a straight line joining sea level at u and v at the i -th profile point is given by:

$$(h_r)_i = (h_u \cdot d_{iv} + h_v \cdot d_{ui}) / d_{uv} \quad (92)$$

$(h_t)_i$, the height of the terrain above a straight line joining sea level at u and v at the i -th profile point is given by:

$$(h_t)_i = h_i + d_{ui} \cdot d_{iv} / 2a_e \quad (93)$$
